Int. J. Heat Mass Transfer. Vol. 25, No. 3, pp. 381–387, 1982
Printed in Great Britain

0017–9310/82/030381–07 $03.00/0
Pergamon Press Ltd.

COLLAPSE OF A CAVITATION BUBBLE BETWEEN TWO SOLID WALLS

G. I. KUVSHINOV, P. P. PROKHORENKO, N. V. DEZHKUNOV
Institute of Applied Physics of the B.S.S.R. Adademy of Sciences, Minsk, U.S.S.R.

and

V. I. KUVSHINOV
Institute of Physics of the B.S.S.R. Academy of Sciences, Minsk, U.S.S.R.

(*Received* 11 *March* 1980 *and in revised form* 10 *June* 1981)

Abstract—A theoretical study is made of the process of cavitation bubble collapse between two solid walls in an ideal incompressible fluid. Following the method developed and running numerical calculations on an electronic computer, the radius and rate of collapse of a cavitation bubble between two solid walls have been determined for different instants of time and angles. The presence of the second solid wall, which brings about a change in the velocity and flow pattern of the added quantity of fluid, is shown to lead to a lesser rate and a markedly different scheme of collapse of cavitation bubbles. These were observed to reduce the erosive activity of acoustic cavitation due to its lesser mechanical attack on the surface and smaller heat transfer from collapsing cavitation bubbles to the surface treated as compared to the case of only one solid wall.

The results obtained, when used to select the optimal conditions for surface treatment, will allow a more effective application of ultrasonic energy in those technological processes which are associated with destructive action of acoustic cavitation resulting from high pressures and heat loads.

NOMENCLATURE

A, $= p_\infty/\rho$;

B, $= p_{in} \cdot R_{max}^4/\rho$;

C_n^m, binomial coefficient;

D_{max}, maximum initial diameter of a cavitation bubble;

$E_{i,n}$, $= r_i^n \cdot P_n(\cos\theta_i)$;

E_n, $= r^n \cdot P_n(\cos\theta)$;

F_n, $= \sum_{m=0}^{\infty} F_{n,m}/l^m$, function which defines the dependence of velocity potential upon time;

G_n, $= \sum_{m=0}^{\infty} \left\{ \frac{F_m C_{m+n}^m}{l^{m+1}} \cdot \sum_{k=1}^{\infty} \left[\frac{(-1)^m + (-1)^n}{(2k-1)^{m+n+1}} + \frac{(-1)^{m+n}+1}{(2k)^{m+n+1}} \right] \right\}$;

l, distance between two parallel solid walls (ultrasonic emitter and solid surface treated);

P_n, Legendre polynomial of order n;

p_b, vapour–gas mixture pressure inside of a bubble;

p_{in}, the value of p_b at time zero, $t = 0$;

p_∞, liquid pressure far from a bubble;

R, instantaneous radius of a cavitation bubble;

R_{max}, maximum initial radius of a cavitation bubble;

R_1, R_2, dimensions of a torus;

r, radial coordinate;

r_i, distance from point O_i (Fig. 1);

T_{in}, temperature in the system "solid surface–liquid–cavitation bubble" at time zero, $t = 0$;

T_b, temperature inside of a cavitation bubble reached at the final stages of its collapse;

t, time;

V_{in}, volume of a cavitation bubble at time zero, $t = 0$;

V_b, volume of a cavitation bubble at final stages of its collapse close to one solid wall;

$\mathbf{v}$, liquid flow velocity;

v_b, rate of cavitation bubble collapse;

$x_{n,m}$, $= R_{n,m}/R_{max}^{n+1}$;

$y_{n,2m}$, $= \frac{dx_{n,2m}}{d\tau}$.

Greek symbols

γ, ratio of heat capacities;

Δ, Laplace operator;

δ, gas content parameter;

θ, angular coordinate;

θ_i, angle (Fig. 1);

λ, $= R_{max}/l$;

ρ, liquid density;

τ, dimensionless time;

φ, liquid flow velocity potential;

∇, Hamiltonian operator.

Subscripts

max, maximum value;

in, refers to the initial instant of time, $t = 0$;

b, refers to bubble;

∞, at a distance from a bubble.

1. INTRODUCTION

MOTION of cavitation bubbles in an infinite liquid and close to one solid wall has been the concern of a number of studies [1–5].

Strong absorption in the region of cavitation rapidly reduces the intensity of sound when it moves away from an ultrasonic emitter. It is for this reason that during hydroabrasive treatment of metals in ultrasonic field, metal coating, ultrasonic cleaning of plane surfaces etc., the surface to be treated is usually brought as close as possible to the emitter. As a result, in technological processes associated with the destructive effect of cavitation there frequently occur situations when a bubble oscillates and actually collapses between two solid walls, i.e. an ultrasonic emitter and a treated solid surface.

At the same time, no practical study has been made of the problem of cavitation bubble collapse between two walls, although it is clear that the hydrodynamic conditions there will differ markedly from the one solid wall case which should affect the erosive activity of acoustic cavitation. This has been proved experimentally [6] at the frequencies 21.7 and 41.9 kHz by measuring a cavitationally induced loss of mass by the specimens vs the distance from an ultrasonic emitter.

It has been established that as the specimen is brought closer to the emitter, it first starts to lose mass monotonically faster and at $l = 0.5\text{–}5.10^{-3}$ m the mass loss reaches the maximum. Then with a further reduction of l the mass loss becomes smaller despite an increase of sound intensity at the specimen surface.

It has been postulated in [6] that a lesser erosive activity of acoustic cavitation on curtailment of the distance l, i.e. when l becomes of the order of maximum initial dimensions of cavitation bubbles D_{max}, is due to a smaller rate of collapse of cavitation bubbles and the absence, under these conditions, of a cumulative jet to a solid surface which is responsible for surface destruction.

The objective of the present research was to theoretically calculate the rate of cavitation bubble collapse between two solid walls and its instantaneous radius and to make a comparison with the case of one solid wall.

2. STATEMENT OF THE PROBLEM: BOUNDARY AND INITIAL CONDITIONS

Consider a cavitation bubble collapsing in a liquid bounded by two parallel solid walls. At time $t = 0$ let the liquid be quiescent, the bubble be spherical and located at the point O a distance $l/2$ from each wall (Fig. 1). The cavitation bubble collapses under constant pressure at infinity, p_∞, so that $p_\infty - p_b > 0$.

Let us make the following assumptions:

(1) the liquid is incompressible and inviscid;

(2) surface tension and gravity force can be neglected;

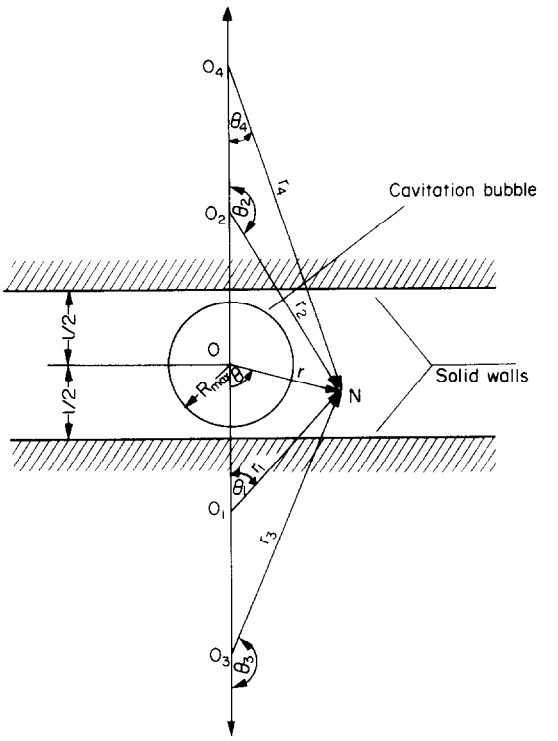

FIG. 1. A cavitation bubble collapsing between two solid walls at time zero, $t = 0$.

(3) compression of the vapour–gas mixture inside of a bubble is adiabatic, with the heat capacity ratio being $\gamma = 4/3$.

It is necessary to determine the radius and rate of cavitation bubble collapse at $t > 0$. The problem will be solved in a spherical system of coordinates $\{r, \theta\}$ with the origin at the point 0.

Presuming the liquid flow to be irrotational ($\nabla \times \mathbf{v} = 0$), introduce the potential $\varphi(r, \theta, t)$ of the liquid flow velocity

$$\mathbf{v} = \nabla\varphi(r, \theta, t).$$

The symmetry of the problem implies the absence of translational motion of a bubble, so it moves only radially.

Based on the above assumptions, the velocity potential $\varphi(r, \theta, t)$ should satisfy the Laplace equation,

$$\Delta\varphi = 0, \tag{1}$$

and the following boundary conditions:

$$\varphi = 0 \text{ at } r \to \infty, \tag{2}$$

$$\frac{\partial\varphi}{\partial r}\cos\theta - \frac{1}{r}\frac{\partial\varphi}{\partial\theta}\sin\theta = 0 \text{ at } r = |l/(2\cos\theta)|, \tag{3}$$

$$\frac{\partial\varphi}{\partial r} - \frac{1}{r^2}\frac{\partial\varphi}{\partial\theta}\frac{\partial R}{\partial\theta} = \frac{\partial R}{\partial t} \text{ at } r = R, \tag{4}$$

$$\frac{\partial\varphi}{\partial t} + \frac{1}{2}\left(\frac{\partial\varphi}{\partial r}\right)^2 + \frac{1}{2r^2}\left(\frac{\partial\varphi}{\partial\theta}\right)^2 = \frac{p_\infty - p_b}{\rho} \text{ at } r = R. \tag{5}$$

The initial conditions are:

$$R = R_{\max}, \quad \frac{dR}{dt} = 0 \text{ at } t = 0.$$

3. VELOCITY POTENTIAL

The velocity potential satisfying equations (1–3) is

$$\varphi = \sum_{n=0}^{\infty} F_n(t)\left[\frac{E_n(r,\theta)}{r^{2n+1}} + \sum_{i=1}^{\infty}\frac{E_{i,n}(r_i,\theta_i)}{r_i^{2n+1}}\right]. \quad (6)$$

Here, the first term within square brackets is due to the hydrodynamic sink [1] located at the point O that replaces the collapsing cavitation bubble, while the second term accounts for the total action of an infinite number of sinks introduced to fulfill the boundary conditions on solid walls and located at the points of reflection relative to these walls, O_i (Fig. 1). In this case the first term in square brackets and the first term in the sum over i correspond to the velocity potential for bubble collapse close to one wall [3].

The quantities $E_n(r,\theta)$ and $E_{i,n}(r_i,\theta_i)$ in (6) are written as

$$E_n(r,\theta) = r^n \cdot P_n(\cos\theta), \quad (7)$$
$$E_{i,n}(r_i,\theta_i) = r_i^n \cdot P_n(\cos\theta_i),$$

while r_i and θ_i can be easily expressed in terms of r, θ, l, i from Fig. 1.

At $r < l$ the functions $E_{i,n}$ satisfy the following relation

$$\frac{E_{i,n}(r_i,\theta_i)}{r_i^{2n+1}} + \frac{E_{i+1,n}(r_{i+1},\theta_{i+1})}{r_{i+1}^{2n+1}} = \begin{cases} \dfrac{1}{[(i+1)l/2]^{n+1}} \displaystyle\sum_{m=0}^{\infty}[(-1)^m + (-1)^n] C_{m+n}^n \left[\frac{r}{(i+1)l/2}\right]^m \cdot P_m(\cos\theta), & i = 1+4k, \\ \dfrac{1}{[(i+1)l/2]^{n+1}} \displaystyle\sum_{m=0}^{\infty}[(-1)^{m+n} + 1] C_{m+n}^n \left[\frac{r}{(i+1)l/2}\right]^m \cdot P_m(\cos\theta), & i = 3+4k, \quad k = 0,1,2,\ldots. \end{cases} \quad (8)$$

Substitution of (8) and (7) into (6) and respective transformation yield:

$$\varphi = \sum_{n=0}^{\infty}\left[\frac{F_n(t)}{r^{n+1}} + G_n(t)\left(\frac{r}{l}\right)^n\right] \cdot P_n(\cos\theta) \quad (9)$$

where

$$G_n(t) = \sum_{m=0}^{\infty}\left\{\frac{F_m(t)\, C_{m+n}^m}{l^{m+1}} \cdot \sum_{k=1}^{\infty} \times \left[\frac{(-1)^m + (-1)^n}{(2k-1)^{m+n+1}} + \frac{(-1)^{m+n}+1}{(2k)^{m+n+1}}\right]\right\}. \quad (10)$$

4. DETERMINATION OF THE RADIUS AND RATE OF CAVITATION BUBBLE COLLAPSE

The instantaneous radius of the cavitation bubble, which characterizes the shape of its surface, can be written as

$$R(\theta,t) = \sum_{m=0}^{\infty} R_m(\theta,t)/l^m,$$

$$R_n(\theta,t) = \sum_{m=0}^{\infty} R_{n,m}(t) \cdot P_m(\cos\theta), \quad R_0 = R_{0,0}. \quad (11)$$

Expand the function $F_n(t)$ into the series

$$F_n = \sum_{m=0}^{\infty} F_{n,m}/l^m, \quad F_{n,0} = 0, \quad F_{0,0} \neq 0. \quad (12)$$

Then, for the term $(p_\infty - p_b)/\rho$ on the right-hand side of (5) one can easily obtain

$$(p_\infty - p_b)/\rho = A - B/R^4,$$
$$A = p_\infty/\rho, \quad B = p_{in} \cdot R_{\max}^4/\rho. \quad (13)$$

In equation (10), for the quantity $G_n(t)$ in the sum over k, let us restrict ourselves to the principal term, which corresponds to the first two reflections

$$G_n = \sum_{m=0}^{\infty}[(1-)^m + (-1)^n] F_m \cdot C_{m+n}^m/l^{m+1}, \quad (14)$$

and neglect small contributions of subsequent reflections.

Then, substituting (9), (11–14) into (4) and (5), assuming $n = 4$ in the resultant equations to simplify calculations [3], separating and setting equal to zero the terms from the 0th to the 4th order in $1/l$, we obtain a system of 10 differential equations of the 1st order for $R_{n,m}$ and $F_{n,m}$. Then, determining and setting equal to zero the coefficients of $P_n(\cos\theta)$ and introducing the dimensionless parameters $x_{n,m} = R_{n,m}/R_{\max}^{n+1}$, $\tau = tA^{1/2}/R_{\max}$, $B/A = p_{in} R_{\max}^4/p_\infty = \delta R_{\max}^4$, $\delta = p_{in}/p_\infty$, $\lambda = R_{\max}/l$, we obtain (omitting all intermediate steps) that $x_{n,2m}\,(2m \geqslant n) = x_{n,2m+1} = 0$, while for x_0 and $x_{n,2m}\,(2m < n), n = 1,2,3,4, m = 0,1,2$—a stationary system of seven 2nd-order ordinary differential equations which, by introducing seven new unknown functions

$$y_0 = \frac{dx_0}{d\tau}, \quad y_{1,0} = \frac{dx_{1,0}}{d\tau}, \quad y_{2,0} = \frac{dx_{2,0}}{d\tau},$$
$$y_{3,0} = \frac{dx_{3,0}}{d\tau}, \quad y_{3,2} = \frac{dx_{3,2}}{d\tau},$$
$$y_{4,0} = \frac{dx_{4,0}}{d\tau}, \quad y_{4,2} = \frac{dx_{4,2}}{d\tau},$$

has been reduced to a system of fourteen 1st-order ordinary differential equations. Knowing the solution of this system, one can determine the instantaneous radius of a cavitation bubble collapsing between two solid walls from the equation

$$R/R_{\max} = x_0 + \sum_{n=1}^{\infty} \lambda_n \times \left[\sum_{m=0}^{k} x_{n,2m} \cdot P_{2m}(\cos\theta) \right], \quad 2k < n \quad (15)$$

and to calculate the rate of its collapse from

$$\frac{\partial}{\partial\tau}(R/R_{\max}) = v_b(p_\infty/\rho)^{-1/2} = y_0 + \sum_{n+1}^{\infty} \lambda^n \times \left[\sum_{m=0}^{k} y_{n,2m} \cdot P_{2m}(\cos\theta) \right], \quad 2k < n. \quad (16)$$

5. RESULTS OF NUMERICAL CALCULATIONS

The stationary system of fourteen 1st-order ordinary differential equations subject to the initial conditions $x_0 = 1, x_{n,2m} = y_0 = y_{n,2m} = 0$ at $\tau = 0$ has been integrated numerically for $\delta = 0$ and $\delta = 0.01$. Then, from the known values of x_0, $x_{n,2m}$, y_0, $y_{n,2m}$ the radius of the cavitation bubble collapsing between two solid walls has been determined by equations (15) and (16) as a function of time τ as well as the rate of its collapse for $\lambda = 1/3, 1/6, 1/10$ and different values of θ. All the calculations were made on an electronic computer "Minsk-32". The results of these calculations are presented in Figs. 2 and 3 and in Tables 1–3. The dashed lines in Figs. 2 and 3 show the respective results obtained in [3] for the case of one solid wall.

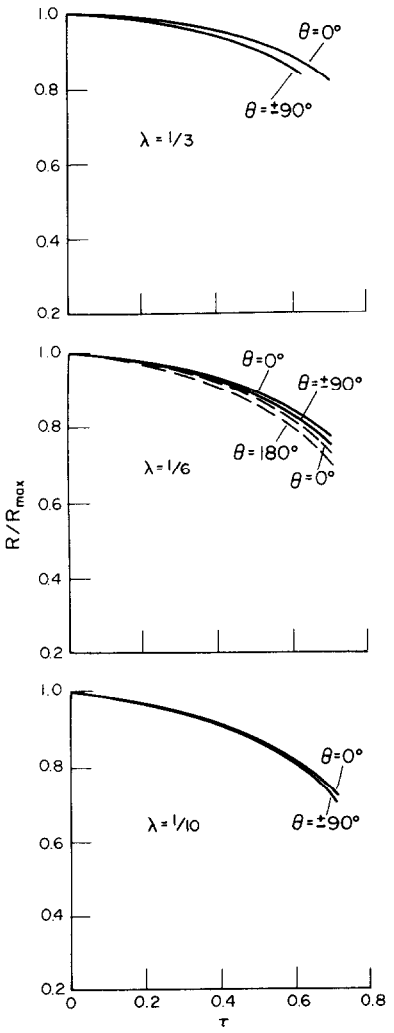

FIG. 2. Collapsing cavitation bubble radius as a function of time at $\delta = 0.01$. Dashed lines correspond to the solution for the one solid wall case [3].

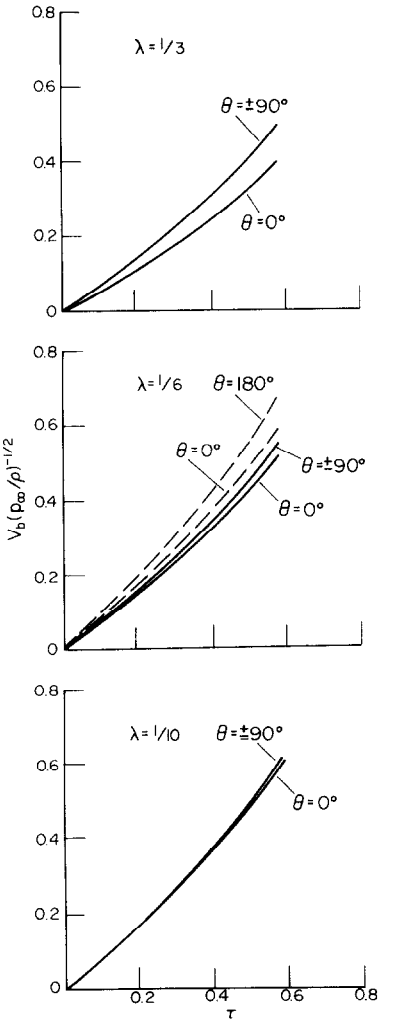

FIG. 3. Rate of cavitation bubble collapse at $\delta = 0.01$. Dashed lines correspond to the solution for the one solid wall case [3].

5.1. *Cavitation bubble radius as a function of time and angle* θ

The time history of the bubble radius is presented in Fig. 2 and Tables 1 and 2 with the angle θ as a parameter. One can see that at the same instant of time the bubble has different radii at different angles θ, i.e. at the time of collapse the bubble is non-spherical and at $\theta = \pm 90°$ its radii are at a minimum.

It also follows from Fig. 2 that the closer the bubble is to the solid walls (the larger is λ), the larger is its radius at the same time instants τ and angles θ.

Table 1. Values of R/R_{max} at $\tau = 0.4$

	λ			1/3		
	θ	0°	±30°(±150°)	±50°(±130°)	±70°(±110°)	±90°
$\delta = 0$	R/R_{max}	0.954	0.950	0.945	0.940	0.938
$\delta = 0.01$	R/R_{max}	0.954	0.951	0.945	0.941	0.939
	λ			1/6		
	θ	0°	±30°(±150°)	±50°(±130°)	±70°(110°	± 90°
$\delta = 0$	R/R_{max}	0.939	0.938	0.937	0.936	0.936
$\delta = 0.01$	R/R_{max}	0.940	0.939	0.938	0.937	0.936
	λ			1/10		
	θ	0°	±30°(±150°)	±50°(±130°)	±70°(±110°)	±90°
$\delta = 0$	R/R_{max}	0.930	0.930	0.930	0.930	0.929
$\delta = 0.01$	R/R_{max}	0.931	0.931	0.931	0.930	0.930

Table 2. Values of R/R_{max} at $\tau = 0.6$

	λ			1/3		
	θ	0°	±30°(±150°)	±50°(±130°)	± 70°(± 110°)	±90°
$\delta = 0$	R/R_{max}	0.882	0.872	0.859	0.848	0.844
$\delta = 0.01$	R/R_{max}	0.884	0.875	0.862	0.851	0.846
	λ			1/6		
	θ	0°	±30°(±150°)	±50°(±130°)	±70°(110°)	±90°
$\delta = 0$	R/R_{max}	0.852	0.850	0.847	0.845	0.844
$\delta = 0.01$	R/R_{max}	0.854	0.852	0.849	0.847	0.846
	λ			1/10		
	θ	0°	±30°(±150°)	±50°(±130°)	±70°(±110°)	±90°
$\delta = 0$	R/R_{max}	0.830	0.830	0.829	0.828	0.828
$\delta = 0.01$	R/R_{max}	0.832	0.832	0.831	0.831	0.830

Table 3. Values of $v_b(p_\infty/\rho)^{-1/2}$ at $\tau = 0.4$

	λ			1/3		
	θ	0°	±30°(±150°)	±50°(±130°)	±70°(±110°)	±90°
$\delta = 0$	$v_b(p_\infty/\rho)^{-1/2}$	0.242	0.263	0.292	0.317	0.327
$\delta = 0.01$	$v_b(p_\infty/\rho)^{-1/2}$	0.239	0.260	0.288	0.313	0.323
	λ			1/6		
	θ	0°	±30°(±150°)	±50°(±130°)	±70°(±110°)	±90°
$\delta = 0$	$v_b(p_\infty/\rho)^{-1/2}$	0.320	0.325	0.331	0.336	0.338
$\delta = 0.01$	$v_b(p_\infty/\rho)^{-1/2}$	0.316	0.321	0.327	0.332	0.334
	λ			1/10		
	θ	0°	±30°(±150°)	±50°(±130°)	±70°(±110°)	±90°
$\delta = 0$	$v_b(p_\infty/\rho)^{-1/2}$	0.367	0.369	0.370	0.372	0.372
$\delta = 0.01$	$v_b(p_\infty/\rho)^{-1/2}$	0.363	0.364	0.366	0.367	0.368

An increase in the gas content δ from 0 to 0.01 retards the process of collapse, as is evident from Tables 1 and 2.

5.2. *Collapse rate of a cavitation bubble*

The calculation results for the bubble collapse rate are presented in Fig. 3 and in Table 3 with the angle θ as a parameter. It follows from Fig. 3 that the collapse rate decreases with increasing λ and rapidly increases with time.

It should be noted that the collapse rates are maximum at $\theta = \pm 90°$, which is in accord with what has been said in Section 5.1 regarding the minimum values of the instantaneous collapsing cavitation bubble radius at these angles.

It is seen from Table 3 that an increase in the gas content δ from 0 to 0.01 leads to a decrease in the rate of collapse.

6. COMPARISON WITH THE ONE SOLID WALL CASE

As is seen from what has been said in Sections 5.1 and 5.2, the presence of the second solid wall substantially alters the pattern of flow of the added mass of liquid on collapse of a cavitation bubble. In this case the instantaneous radii of a cavitation bubble are minimum, while the collapse rates are maximum, at $\theta = \pm 90°$. This scheme of cavitation bubble collapse differs markedly from that observed in the vicinity of one solid wall when the instantaneous radii of a cavitation bubble are minimum, while the collapse rates are maximum, at $\theta = 180°$ (dashed lines in Figs. 2 and 3) which eventually leads to the formation of a cumulative jet directed to the solid wall [5].

In addition, the presence of the second solid wall deteriorates the conditions of liquid inflow to a collapsing cavitation bubble, and the flow velocity of the added mass of liquid decreases. This leads to a

decrease of the rate of cavitation bubble collapse and to an increase of the time of its collapse as compared with the case of one solid wall (Figs. 2 and 3).

Thus, the second solid wall markedly changes the main characteristics of the process of collapse of cavitation bubbles and, consequently, their erosive activity.

6.1. *Mechanical effect of acoustic cavitation*

The magnitude of the erosive activity of acoustic cavitation can, first of all, be affected by a change in the mechanical action of high-speed cumulative microjets of liquid originating during collapse of cavitation bubbles. As follows from the above results of numerical calculations, the cavitation bubbles located between two solid walls (a treated surface and an ultrasonic emitter) at a distance $l/2 \sim R_{max}$ from each wall collapse without forming such jets. This may decrease the mechanical effect of acoustic cavitation as compared with the one solid wall case.

A lower rate of collapse, established above, may also be the reason for a decrease in the destructive action of acoustic cavitation on the treated solid surface due to a diminished mechanical effect in the case considered.

6.2. *Thermal effect of acoustic cavitation*

A change in the velocity and pattern of the added liquid mass flow on cavitation bubble collapse in the space between two parallel solid walls may also lead to a change in the thermal effect of acoustic cavitation on the solid surface treated.

By thermal effect of acoustic cavitation we mean heating of a solid wall close to which cavitation bubbles collapse. It is due mainly to conversion into heat of the mechanical work of cavitation on the interaction of bubbles with the solid surface and also to heat transfer from collapsing cavitation bubbles to a solid surface.

Since the second solid wall diminishes the mechanical effect of acoustic cavitation, it may also reduce the thermal effect which is due to conversion into heat of mechanical work done by high-speed cumulative microjets of liquid responsible for destruction of the solid surface treated.

Heat transfer from a collapsing cavitation bubble to the solid surface is attributed to very high temperatures originating inside of a bubble in the process of its adiabatic collapse. Thus, when a non-spherical bubble collapses with formation of a cumulative jet, the vapour–gas mixture inside of it is heated up to the average maximum temperature

$$T_b = T_{in}\left(\frac{V_{in}}{V_b}\right)^{\gamma-1}. \qquad (17)$$

Taking into account that the initial volume of a cavitation bubble, $V_{in} = 4/3\pi R_{max}^3$, and the volume V_b being equal in this case to the volume of a torus whose form is acquired by the bubble at the final stages of collapse, $V_b = (\pi^2/4)(R_1 + R_2)(R_1 - R_2)^2$, and assuming $R_1 \simeq 0.2\,R_{max}$, $R_2 \simeq 0.1\,R_{max}$ [5], $T_{in} = 300$ K, we obtain from equation (17)

$$T_b \simeq 2500\,\text{K}.$$

When a cavitation bubble collapses between two solid walls, then, due to non-uniformity of vapour–gas mixture compression, the zone of maximum temperatures inside of a bubble will obviously be located in the region $\theta \sim \pm 90°$, while in the case of one solid wall, in the region $\theta \sim 180°$ (at the tip of a cumulative jet), i.e. at $l \sim D_{max}$, directly near the solid surface treated.

Moreover, in the case of two solid walls heat is also transferred from a collapsing cavitation bubble to the second solid wall (to the surface of an ultrasonic emitter). These circumstances may reduce thermal effect of acoustic cavitation which is contributed by heat transfer from a collapsing cavitation bubble to the solid surface treated.

Thus, the second solid wall reduces the mechanical and thermal effects of acoustic cavitation and diminishes its erosive activity, which is consistent with the experimental data of [6].

What has been said above confirms also the hypothesis advanced in [6] regarding the reasons for reduced erosive activity of acoustic cavitation in the space between an ultrasonic emitter and a solid surface with a decrease of l, i.e. at $l \sim D_{max}$.

7. CONCLUSIONS

(1) The procedure has been developed for theoretical calculation of the radius and rate of collapse of a cavitation bubble between two solid walls in an ideal incompressible liquid on the assumption that the surface tension and gravity force may be neglected, while the vapour–gas mixture inside of a bubble is compressed following the adiabatic law.

Based on the theory developed, a change in time of the radius and rate of collapse of a cavitation bubble have been calculated.

(2) It is shown that at large values of λ ($> 1/10$) the shape of a collapsing cavitation bubble differs markedly from the initial spherical one. At $\lambda = 1/10$ the collapsing bubble is practically spherical.

(3) It has been found that with increasing λ the rate of collapse of a bubble decreases, while the time of collapse increases, with the collapse rates being maximum, and the radii minimum, at the same time instant at $\theta = \pm 90°$.

(4) It has been established that an increase in the gas content parameter from 0 to 0.01 decelerates collapse of a cavitation bubble.

(5) It is shown that at $l \sim D_{max}$ the second wall, which alters the pattern and velocity of flow of the added mass of liquid, also causes a substantial change in the very scheme of cavitation bubble collapse and decreases the rate of collapse as compared with the one solid wall case. These factors may influence the erosive activity of acoustic cavitation, reducing it due to (along with other reasons) smaller mechanical effect of acous-

tic cavitation and heat transfer from collapsing cavitation bubbles to the solid surface treated. This conclusion agrees with the available experimental results.

REFERENCES

1. R. H. Cole, *Underwater Explosions*. Princeton, New Jersey (1948).
2. W. P. Mason (editor), *Physical Acoustics, Principles and Methods. Vol. 1, Methods and Devices, Part B*. Academic Press, New York (1964).
3. A. Shima, The behaviour of a spherical bubble in the vicinity of a solid wall. *Trans. ASME, Ser. D, J. basic Engng* **90**, 84–99 (1968).
4. L. D. Rozenberg (editor), *High-Power Ultrasonic Fields*. Nauka Press, Moscow (1968).
5. O. V. Voinov and V. V. Voinov, Concerning the scheme of cavitation bubble collapse at the wall and formation of a cumulative jet, *Dokl. Akad. Nauk S.S.S.R.* **207**, 63–66 (1976).
6. P. P. Prokhorenko, N. V. Dezhkunov and G. I. Kuvshinov, Towards optimization of ultrasonic technological processes in liquids, *Izv. Akad. Nauk B.S.S.R., Ser. Fiz.-Tekh. Nauk No. 1*, 71–73 (1979).

COLLAPSUS D'UNE BULLE DE CAVITATION ENTRE DEUX PAROIS SOLIDES

Résumé—On étudie par voie théorique le mécanisme du collapsus d'une bulle de cavitation entre deux parois solides dans un fluide incompressible idéal. Les calculs numériques sur ordinateur déterminent, pour différents instants et plusieurs angles, le rayon et la vitesse du collapsus. La présence de la seconde paroi modifie la vitesse et la configuration de l'écoulement et conduit à une diminution de la vitesse de collapsus et à une évolution nettement différente. Elle réduit l'activité érosive de la cavitation acoustique du fait d'une attaque mécanique moindre de la surface et le transfert thermique est plus faible par rapport au cas de bulle de cavitation qui collapse en présence d'une seule paroi solide.

Les résultats obtenus, lorsqu'ils correspondent aux conditions optimales de traitement de surface, conduisent à une application plus efficace de l'énergie ultrasonore dans les procédés technologiques qui sont associés à l'action destructrice de la cavitation acoustique à pression élevée et à forte charge.

DAS ZUSAMMENBRECHEN EINER KAVITATIONSBLASE ZWISCHEN ZWEI FESTEN WÄNDEN

Zusammenfassung—Das Zusammenbrechen von Kavitationsblasen in einer idealen inkompressiblen Flüssigkeit zwischen zwei festen Wänden wird theoretisch untersucht. Mittels des entwickelten Verfahrens und numerischer Berechnungen wurden Radius- und Zusammenbruchs-Geschwindigkeit einer Kavitationsblase zwischen zwei festen Wänden für verschiedene Zeiten und Winkel bestimmt. Das Vorhandensein der zweiten Wand, das eine Änderung der Geschwindigkeit und der Strömungsform der zugeführten Flüssigkeit bedingt, führt zu einer Geschwindigkeitsverringerung und zu einem merklich veränderton Ablauf des Zusammenbrechens von Kavitationsblasen. Verglichen mit dem Fall nur einer festen Wand resultiert daraus eine Abnahme der Erosionswirkung der akustischen Kavitation aufgrund des verringerten mechanischen Angriffs und Wärmeübergangs von der zusammenbrechenden Kavitationsblase auf die behandelte Oberfläche.

Bei der Auswahl optimaler Bedingungen zur Oberflächenbehandlung ermöglichen die erhaltenen Ergebnisse eine wirkungsvollere Anwendung der Ultraschall-Energie in den technologischen Prozessen, die mit der zerstörenden Einwirkung akustischer Kavitation aufgrund hoher Drüke and Wärmebelastungen verbunden sind.

ЗАХЛОПЫВАНИЕ КАВИТАЦИОННОГО ПУЗЫРЬКА МЕЖДУ ДВУМЯ ТВЕРДЫМИ СТЕНКАМИ

Аннотация — Проведено теоретическое исследование процесса захлопывания кавитационного пузырька между двумя твердыми стенками в идеальной несжимаемой жидкости. На основе разработанной методики путем численных расчетов на ЭВМ для различных моментов времени и углов были вычислены радиус и скорость захлопывания кавитационного пузырька между двумя твердыми стенками. Показано, что наличие второй твердой стенки, вызывающее изменение скорости потока присоединенной массы жидкости и характера ее движения, приводит к уменьшению скорости захлопывания кавитационных пузырьков и существенному изменению самой схемы их захлопывания. Отмечено, что указанные обстоятельства снижают эрозионную активность акустической кавитации за счет уменьшения ее механического воздействия и снижения теплопереноса от захлопывающихся кавитационных пузырьков к обрабатываемой поверхности по сравнению со случаем одной твердой стенки.

Учет полученных в данной работе результатов при выборе оптимальных режимов обработки позволит более эффективно использовать ультразвуковую энергию в технологических процессах, связанных с разрушающим действием акустической кавитации, которое обусловлено высокими давлениями и тепловыми нагрузками.